Available online at www.sciencedirect.com

ScienceDirect

Solar Energy 125 (2016) 453–459

SOLAR ENERGY

www.elsevier.com/locate/solener

Optical properties and thermal stability of colored solar selective absorbing coatings with double-layer antireflection coatings

Ruihua Yang [a,c], Jinyang Liu [a,b,*], Limei Lin [a,b], Yan Qu [a], Weifeng Zheng [a], Fachun Lai [a,b,*]

[a] College of Physics and Energy, Fujian Normal University, Fuzhou 350108, PR China
[b] Fujian Provincial Key Laboratory of Quantum Manipulation and New Energy Materials, Fuzhou 350108, PR China
[c] Foctek Photonics, Inc., Fuzhou 350108, PR China

Received 5 July 2015; received in revised form 25 November 2015; accepted 15 December 2015

Communicated by: Associate Editor Yanjun Dai

Abstract

Multilayer solar selective absorbing coatings of $Cu/Ti/SiO_2/Ti/TiO_2/SiO_2$ were designed first and then deposited on quartz substrates using the magnetron sputtering method. The thicknesses of the individual layers were optimized to achieve high solar absorptance, while the colors were designed with the TFCalc optical design software. The colors of the coatings including purple, blue, blue green, yellow green and orange yellow were prepared based on the designed parameter. The colored solar selective absorbing coatings exhibit solar absorptance higher than 0.95 and thermal emissivity lower than 0.09 at 80 °C. Furthermore, the thermal stability of the $Cu/Ti/SiO_2/Ti/TiO_2/SiO_2$ coatings was studied by annealing at high temperature in vacuum and in air for 2 h. The X-ray diffraction, X-ray photoelectron spectroscopy, Raman spectroscopy and spectrophotometry were used to characterize properties of the coatings. The results showed that the multilayer solar selective absorbing coatings were thermally stable at 450 °C in vacuum and 300 °C in air for 2 h, which may provide an instruction to design and fabricate high performance colored solar selective absorbing coatings.

Keywords: Solar absorbing coating; High solar absorptance; Colored; Thermal stability

1. Introduction

Recently, there is an urgent need to develop a versatile strategy to make use of the renewable clean energy due to the environmental pollution and ecological destruction resulted from a large amount of fossil energy consumption of the world. As a kind of universal, huge reserves and pollution-free energy, solar energy has gained great attention. At present, lots of approaches have been explored to make use of solar energy, such as solar-thermal conversion and photoelectric conversion technology. The solar-thermal conversion technology is a simple, direct energy conversion method with long utilization history. The solar selective absorbing coating is the main part of solar-thermal conversion device, whose performance plays a crucial role in solar-thermal conversion efficiency and further application (Selvakumar and Barshilia, 2012). In order to improve the energy conversion efficiency, the solar selective absorbing coatings should be designed to have a lower reflection in the solar spectrum region, while contain a

* Corresponding authors at: College of Physics and Energy, Fujian Normal University, Fuzhou 350108, PR China. Tel.: +86 591 22868137; fax: +86 591 22868132.
E-mail addresses: jyliu@fjnu.edu.cn (J. Liu), laifc@fjnu.edu.cn (F. Lai).

http://dx.doi.org/10.1016/j.solener.2015.12.022
0038-092X/

higher reflection in the infrared wavelength region (Kanu and Binions, 2009; Bostrom et al., 2003).

Now, several types of structure have been proposed to gain the high performance solar selective absorbing coatings, such as metal/dielectric multilayer coatings of Al/AlN/Al/AlN (Chen et al., 2011), metal-dielectric composite coatings of Mo–SiO_2 (Zheng et al., 2015). In the solar selective absorbing coatings, the antireflective (AR) coatings play an excellent role on the performance of solar absorptance. To obtain optimum absorptance, the AR coatings should be adopted to produce a minimum reflectance in the visible region, in which possess largest amount of the solar energy (Schüler et al., 2005). Generally, a low-index layer and a higher-index layer were adopted to construct the AR coating based on interferential theory. Due to their excellent chemical inertness and favorable optical property, the AR coatings constructed with TiO_2 and SiO_2 layers have been extensively studied. For example, Li et al. (2014) reported that the TiO_2–SiO_2 stack coatings increased the efficiency of CIGS solar cells. Lien et al. (2006) reported that a 39% enhancement in conversion efficiency was obtained in the single crystalline Si solar cell with SiO_2/SiO_2–TiO_2 mixture/TiO_2 triple-layer AR coatings. Ye et al. (2013) reported the SiO_2/TiO_2/SiO_2–TiO_2 mixture triple-layer coatings with an average transmittance of more than 98.4% for solar cell cover glass. In addition to improving the conversion efficiency, the AR coatings were used to control the color appearance of the solar absorber. Boudaden et al. (2005) studied multilayered Al_2O_3/SiO_2 and TiO_2/SiO_2 coatings deposited on glass substrates as a colored glazed cover for thermal solar collectors and buildings. As the consumption of the solar-thermal conversion device increasing, it becomes a very interesting project to integrate solar-thermal collectors into buildings (Wang and Zhai, 2010; Anderson et al., 2010; Tripanagnostopoulos et al., 2000).

In this report, the Cu/Ti/SiO_2/Ti/TiO_2/SiO_2 multilayer solar selective absorbing coating was designed and fabricated based on the metal/dielectric multilayer interference stack concept. In the structure, the Cu was designed for infrared reflective layer due to its low-emissivity, the transition metal Ti was used as absorbing layer due to its inherent spectral selectivity and excellent thermal stability, while the double-layer TiO_2/SiO_2 AR coatings were utilized to improve the conversion efficiency and control the colors together with other layers, which is rarely reported so far. Numerical simulation allows optimizing and obtaining the colored multilayer coatings using TFCalc optical design software. The crystal structure, chemical composition, Raman vibration mode and optical property of the multilayer solar selective absorbing coating were characterized by X-ray diffraction (XRD), X-ray photoelectron spectroscopy (XPS), Raman spectroscopy and spectrophotometry, respectively. Furthermore, the thermal stability of the multilayer solar selective absorbing coatings by annealing at high temperature in vacuum and in air has been studied.

2. Experimental details

The Cu/Ti/SiO_2/Ti/TiO_2/SiO_2 multilayer solar selective absorbing coatings were deposited on quartz substrates ($25 \times 25 \times 0.5\ mm^3$) with the magnetron sputtering system without additional heating. The chamber was pumped down to 4.0×10^{-4} Pa before the deposition. The Ti and Cu films were deposited from direct current (DC) sputtering of Ti (4N purity) and Cu (4N purity) targets, respectively, in Ar (5N purity, 40 sccm) at 0.5 Pa with 100 W. The dielectric SiO_2 films were prepared from the reactive radio-frequency (RF) sputtering of Si target (4N purity) in Ar (5N purity, 40 sccm) + O_2 (5N purity, 5 sccm) at 0.3 Pa with 120 W. The dielectric TiO_2 films were prepared from the reactive DC sputtering of Ti target in Ar (5N purity, 40 sccm) + O_2 (5N purity, 7 sccm) at 0.3 Pa with 150 W. The substrates were rotated at a speed of 30 rpm above the targets in a distance of 130 mm during the deposition process to improve the uniformity. The thickness of the Cu layer was about 150 nm, making the Cu/Ti/SiO_2/Ti/TiO_2/SiO_2 multilayer coatings was almost zero transmittance.

The reflectance (R) and transmittance (T) of the coatings were measured with a double-beam spectrophotometer (Perkin–Elmer Lambda 950) in the wavelength range of 300–2500 nm, while the infrared reflectance was recorded by a Fourier transform infrared (FTIR) spectrophotometer (Perkin Elmer Spectrum One) in the wavelength range of 2.5–25 μm. The solar absorptance (α) was calculated by numerical integration using the measured reflectance data with an integrating sphere and the solar irradiance at AM 1.5 in the wavelength range of 300–2500 nm, while the thermal emissivity (ε) was calculated from the measured reflectance data and the blackbody spectral radiation at 80 °C in the wavelength range of 2.5–50 μm assuming that the reflectance at the wavelength larger than 25 μm was the same as the reflectance at 25 μm (Wu et al., 2013; ISO, 1994). For each sample, three reflectance spectra were measured from different positions within the coating to obtain mean values of solar absorptance and thermal emissivity, and the evaluated mean values were used in the subsequent data analysis.

In the CIE (International Commission on Illumination) color system, the color of coating was numerically represented on CIE1931 chromaticity diagram, and the color coordinates x and y of coating can be calculated from its measured reflectance data without an integrating sphere and the standard spectrum tristimulus values (Zhu and Zhao, 2010). The brightness of coating surface is determined by its visible reflectance R_{vis}, which is derived from the photopic luminous efficiency function, the standard illumination D65 and the reflectivity of coatings (Zheng et al., 2012). The color difference, ΔE^*_{uv} between two color stimuli is calculated as the Euclidean distance between the points representing them in CIE1976 (L^*, u^*, v^*) color space (Kasson and Plouffe, 1992).

In order to study the thermal stability, the typical coatings of Cu/Ti/SiO_2/Ti/TiO_2/SiO_2 deposited on quartz substrates with blue appearance were annealed at 400 °C, 450 °C, 500 °C and 550 °C (the heating/cooled down rate is 3 °C/min) for 2 h in vacuum (8×10^{-4} Pa), respectively. The thermal stability of the coatings in air was also studied with the similar procedure.

The X-ray diffraction (XRD) (MiniFlex II diffractometer, Cu $K\alpha$, $\lambda = 1.5418$ Å, 30 kV, 15 mA) was used to characterize the crystal structure. The X-ray photoelectron spectroscopy (XPS) (ESCALAB 250 X-ray photoelectron spectroscopy system, Al Kα, $E = 1486.6$ eV) was used to characterize the chemical composition. The Raman spectroscopy (Horiba JY Evolution, 532 nm, 100×) was used to study the vibration mode of the materials.

3. Results and discussion

3.1. Optical constants of SiO_2, TiO_2 and Ti films

The optical constants (refractive index (n) and extinction coefficient (k)) are fundamental parameters for the simulation of the spectroscopic characteristics of the optical multilayer film. In this work, the optical constants of dielectric SiO_2 and TiO_2 were calculated from the experimental transmittance spectra by the Forouhi–Bloomer model combined with the modified Drude model (Wu et al., 2013; Lai et al., 2007). The optical constants of metal Ti film were calculated from the experimental reflectance and transmittance spectra by the Drude–Lorentz model (Wu et al., 2013). Fig. 1a shows the transmittance spectra of SiO_2, TiO_2 and Ti films and the reflectance spectra of Ti film on quartz substrates. The solid lines are the measured spectra, and the dotted lines are the calculated spectra. It can be seen that the experimental spectra are in good agreement with the calculated results. The obtained optical constants of these films in the range of 300–2500 nm are shown in Fig. 1b. The results indicate that SiO_2 and TiO_2 act as antireflection layer, and transition metal Ti acts as absorbing layer in the solar selective absorbing coatings.

3.2. Design and characterization of Cu/Ti/SiO_2/Ti/TiO_2/SiO_2 coating

The Cu/Ti/SiO_2/Ti/TiO_2/SiO_2 structure based on the metal/dielectric multilayer interference mechanism was adapted to the solar selective absorbing coating. In the structure, the double-layer TiO_2/SiO_2 acts as antireflection layers, the Cu layer works as infrared reflector layer, while the Ti layer works as absorbing layer, and the SiO_2 layer between Ti layers acts as optical spacer. The solar selective absorbing coatings with high performance and colors were designed by TFCalc optical design software based on optical constants of the materials with metal/dielectric multilayer structure and then deposited on quartz substrates using the magnetron sputtering method. The simulation results show that all the colored coatings of Cu/Ti/SiO_2/Ti/TiO_2/SiO_2 exhibit the solar absorptance higher than 0.95 and thermal emissivity lower than 0.09 at 80 °C. The crystal structure of the typical coating with blue appearance was characterized by the XRD and the results are shown in Fig. 2. According to JCPDS international diffraction database (ICDD), it is found that the peak at 43.44° corresponds to the Cu (1 1 1) plane. The peaks at 50.73° and 74.42° correspond to the (2 0 0) and (2 2 0) planes of Cu, respectively. It maybe due to the thickness of the TiO_2 and SiO_2 layers was very thin and the deposition temperature was low (at room temperature), so the crystallinity was very bad, subsequently, no diffraction peaks of the Ti, TiO_2 and SiO_2 were observed in XRD data.

3.3. Colored solar selective absorbing coatings

Due to the fact that the reflectivity of the multilayer coating relies on the film thicknesses of the different layer based on the optical thin film characteristic matrix theory, the different colors of the Cu/Ti/SiO_2/Ti/TiO_2/SiO_2 solar selective absorbing coatings can be obtained by controlling the thickness of the different layer. Table 1 lists the thickness of the different layers of the coatings with different colors including purple, blue, blue green, yellow green and

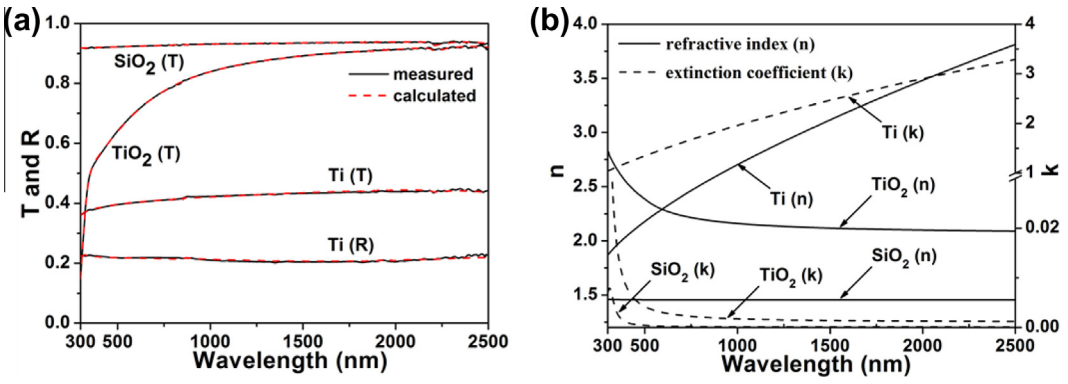

Fig. 1. (a) The transmittance spectra (T) of SiO_2, TiO_2 and Ti films and the reflectance spectrum (R) of Ti film on quartz substrates. (b) The obtained values of n (solid lines) and k (dotted lines) of SiO_2, TiO_2 and Ti films.

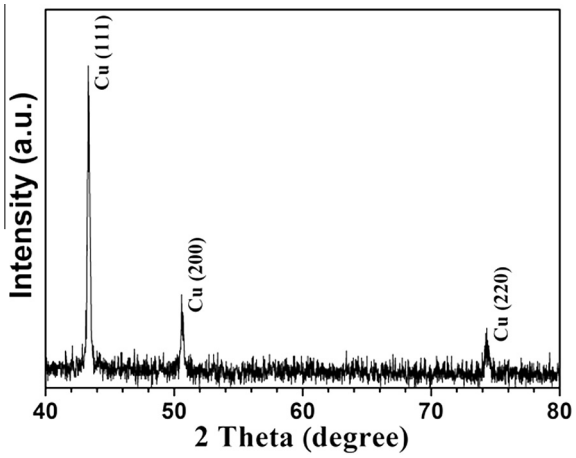

Fig. 2. XRD pattern of the Cu/Ti/SiO_2/Ti/TiO_2/SiO_2 coating deposited on quartz substrate.

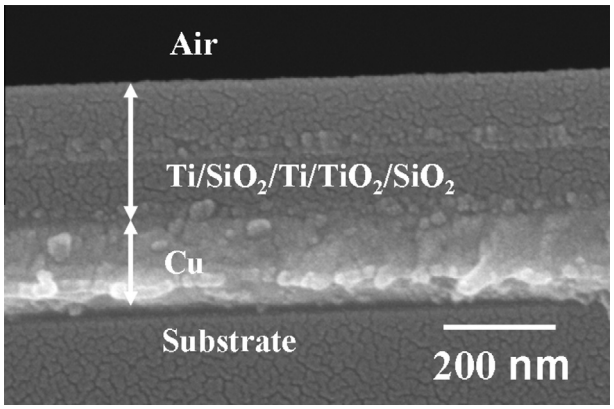

Fig. 3. Cross section SEM images of the blue coating of Cu/Ti/SiO_2/Ti/TiO_2/SiO_2 on quartz substrate.

orange yellow simulated by the TFCalc optical design software based on the optical constants. Then the coatings with different colors were deposited on quartz substrates according to the corresponding thickness designed using the magnetron sputtering method. At first, we obtained the average sputtering ratio of the layer by measuring the cross section SEM image of the coatings deposited on quartz substrates with different deposition time in the same condition. Then the different layers of the color coatings were deposited with the designed thickness based on the average sputtering ratio. Fig. 3 shows the typical cross section of blue coating characterized by SEM, it constructed with Ti/SiO_2/Ti/TiO_2/SiO_2, and the designed thickness of the layers were 24 nm, 69 nm, 21 nm, 26 nm and 92 nm, respectively, the total thickness was 232 nm. From the image, the interface between each layer cannot be distinguished clearly, but the total thickness is about 235 nm, which is consisted with the simulated results (232 nm).

The reflectance spectra and color appearances (the picture insets) are shown in Fig. 4, furthermore, the color locations from Fig. 4a–e are marked by "Purple", "Blue", "Blue Green", "Yellow Green" and "Orange Yellow" on the CIE1931 chromaticity diagram (Fig. 4f), respectively. The values of x and y of coatings were calculated from experimental reflectance spectra refer to ISO 11664-1. Color coordinates x and y, solar absorptance, thermal emissivity and brightness of the colored solar selective absorbing coatings are also listed in Table 1. It can be seen that the solar absorptance are higher than 0.95 and the thermal emissivity are lower than 0.09 at 80 °C in all colored coatings.

3.4. Thermal stability in vacuum

In order to explore the thermal stability, the typical coatings of Cu/Ti/SiO_2/Ti/TiO_2/SiO_2 with blue appearance were annealed at 400 °C, 450 °C, 500 °C and 550 °C in vacuum for 2 h, respectively. Table 2 shows the typical parameters, such as absorptance, emissivity, color coordinates, brightness R_{vis} and color change ΔE^*_{uv} of the coatings on the basis of the reflectance spectra. It clearly shows that no significantly change can be found after annealing at 450 °C. However, there is little change in the absorptance and emissivity after annealing at 500 °C. And the $\Delta\alpha$, $\Delta\varepsilon$ and color change ΔE^*_{uv} increase gradually as the annealing temperature increases. The poor solar selectivity (α/ε) and a big color change ($\Delta E^*_{uv} = 14.48$) were appeared after annealing at 550 °C, indicating the coating cannot be operated at this temperature.

In addition, the Raman spectra of the coatings (Fig. 5) shows the same trend. No obvious band shift can be observed for the coating annealed at 450 °C. However, weak peaks located at around 218 and 308 cm^{-1} corresponded to Cu_2O were appeared after annealing at 500 °C (Solache-Carranco et al., 2008). After annealing at the higher temperature (550 °C), the peak located at 308 cm^{-1} disappeared, whereas, the peak located at 218 cm^{-1} enhanced. Furthermore, based on the escape

Table 1
Thickness for each layer, color coordinates x and y, solar absorptance (α), thermal emissivity (ε), and brightness of colored solar selective absorbing coatings of Cu (150 nm)/Ti/SiO_2/Ti/TiO_2/SiO_2.

Colored coatings	d [Ti/SiO_2/Ti/TiO_2/SiO_2] (nm)	(x, y)	α	ε	R_{vis} (%)
Purple	18/55/21/30/85	(0.25, 0.10)	0.956	0.085	0.38
Blue	24/69/21/26/92	(0.19, 0.21)	0.963	0.081	1.71
Blue Green	23/84/22/43/87	(0.21, 0.30)	0.957	0.086	1.88
Yellow Green	24/64/30/35/95	(0.38, 0.47)	0.951	0.078	2.91
Orange Yellow	20/41/21/37/72	(0.51, 0.45)	0.950	0.089	2.18

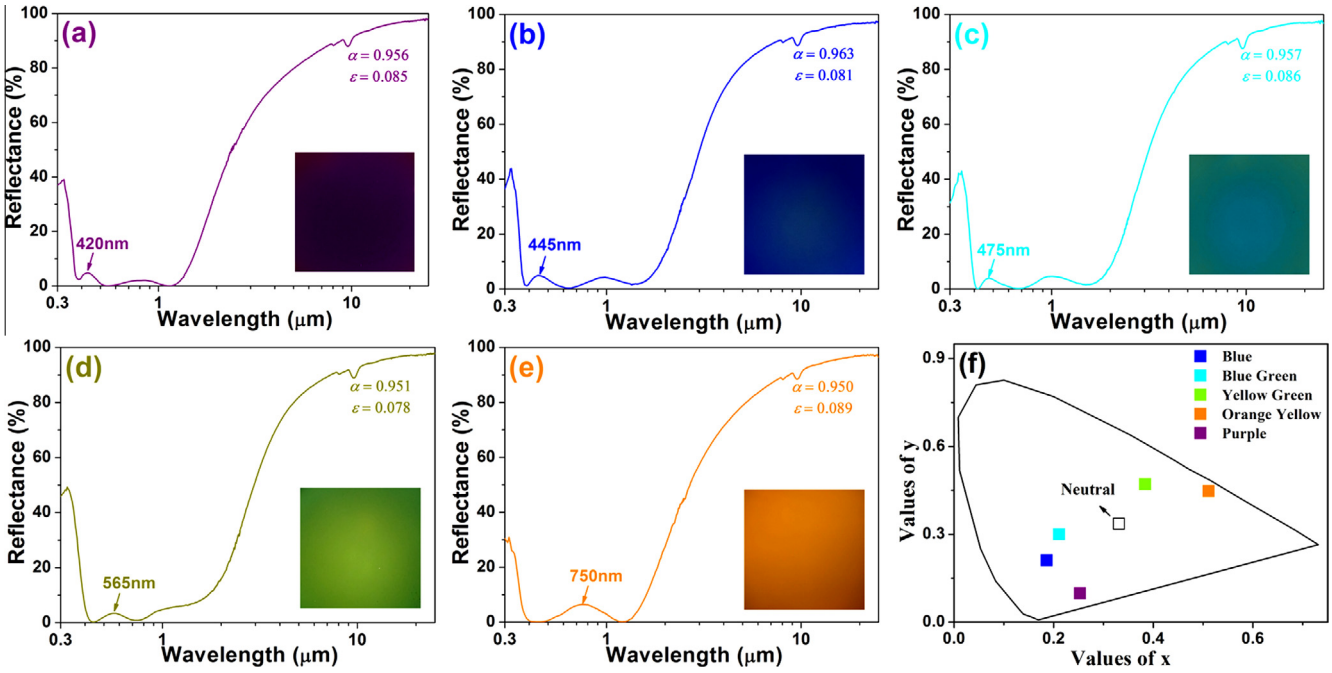

Fig. 4. The reflectance spectra of colored solar selective absorbing coatings with (a) purple, (b) blue, (c) blue green, (d) yellow green, (e) orange yellow appearance, and (f) the chromaticity diagram of colored coatings. Insets are the color appearances of the coatings. (For interpretation of the references to colour in this figure legend, the reader is referred to the web version of this article.)

Table 2
Effect of 2 h annealing in vacuum on the absorptance (α), emissivity (ε) and color change (ΔE^*_{uv}) of the blue coatings.

Annealing temperature (°C)	As-deposited		Annealed		Δα	Δε	ΔE^*_{uv}
	α	ε	α′	ε′			
400	0.964	0.078	0.964	0.086	0.000	0.008	1.38
450	0.965	0.080	0.959	0.089	−0.006	0.009	3.41
500	0.966	0.081	0.948	0.092	−0.018	0.011	9.07
550	0.964	0.076	0.917	0.101	−0.047	0.025	14.48

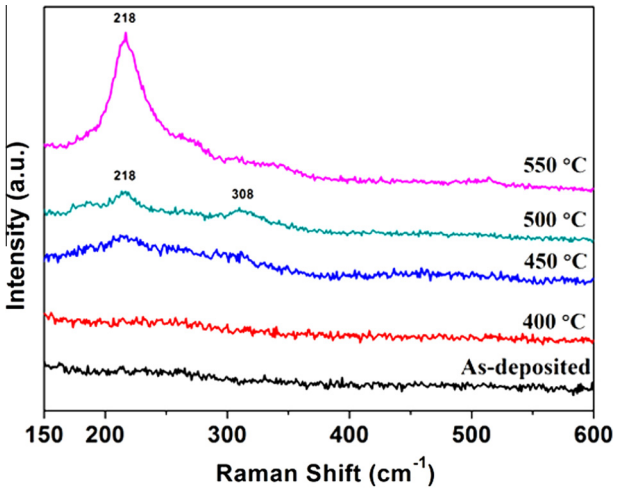

Fig. 5. The Raman spectroscopy of the Cu/Ti/SiO_2/Ti/TiO_2/SiO_2 coatings before and after annealing from 400 °C to 550 °C in vacuum for 2 h.

depth of the photoelectrons is not larger than 10 nm, the XPS was used to analyze the actual chemical composition of the Cu (150 nm)/Ti (24 nm) coatings annealed at 450 °C, 500 °C and 550 °C in vacuum for 2 h. As previous reports, the peaks located at 932.6 eV and 952.2 eV are originated from Cu $2p_{3/2}$ and Cu $2p_{1/2}$ electrons in metallic Cu, respectively (Tahir and Tougaard, 2012; Biesinger et al., 2010). No characteristic peaks related to Cu can be found in the as-deposited and the coating annealing at 450 °C. While the weak Cu signal was identified in the coating after annealing at 500 °C and that the relatively strong peaks were stretched out at the higher temperature (550 °C), as demonstrated in Fig. 6. Therefore, the results show that the Ti layer is able to prevent the Cu diffusion up to 450 °C, however, the Cu diffuses when the annealed temperature is higher than 500 °C. So, it can be concluded that the degradation of Cu/Ti/SiO_2/Ti/TiO_2/SiO_2 coatings at temperature higher than 500 °C is accounted to the diffusion of copper and subsequently oxidized with oxygen came from the SiO_2 layer.

3.5. Thermal stability in air

Thermal stability of the solar selective absorbing coating in air is also very important in case the vacuum is breached.

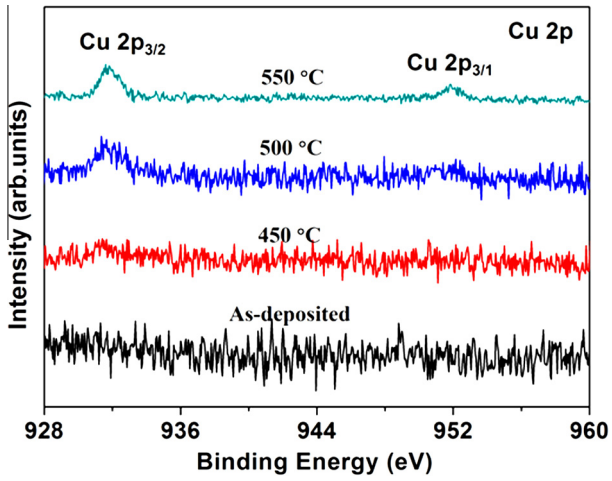

Fig. 6. The XPS spectra of Cu 2p peak for Cu/Ti coatings before and after annealing from 400 °C to 550 °C in vacuum for 2 h.

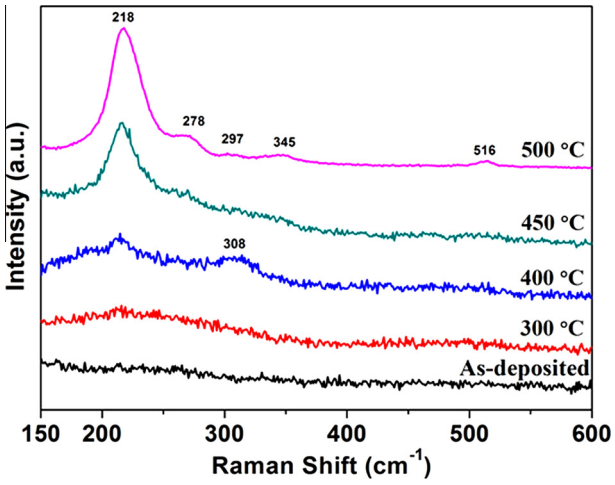

Fig. 7. The Raman spectroscopy of the $Cu/Ti/SiO_2/Ti/TiO_2/SiO_2$ coatings before and after annealing from 400 °C to 500 °C in air for 2 h.

In order to test the thermal stability of the blue coatings of $Cu/Ti/SiO_2/Ti/TiO_2/SiO_2$ in air, the coatings were annealed at temperatures in the range of 300–500 °C for 2 h. Table 3 gives the corresponding absorptance, emissivity, color coordinates, brightness R_{vis} and color change ΔE^*_{uv} of the multilayer coatings. It can be seen from Table 3 that no significantly change can be found in the optical properties of the coating annealed at 300 °C in air. However, the optical properties degenerated gradually which is found from the increase of their emissivity and color change ΔE^*_{uv}, and the larger degradation occurred in air than in vacuum by the heat treatment.

Raman spectroscopy is an excellent method to characterize the change of the coatings before and after annealing, and the results are shown in Fig. 7. It is shown that no obvious band shift can be observed in the annealed coating up to 300 °C in air. However, at 400 °C, weak peaks located at around 218 and 308 cm^{-1} originated from Cu_2O were found in the coating. And some peaks located at around 218, 278, 297, 345 and 516 cm^{-1} appeared after annealing at 500 °C. The bands centered at 218 and 516 cm^{-1} correspond to Cu_2O (Solache-Carranco et al., 2008), whereas bands centered at 297 and 345 cm^{-1} correspond to CuO (Chrzanowski and Irwin, 1989), and the band centered at 278 cm^{-1} corresponds to Ti_2O_3 (Nemanich et al., 1980; Arsov et al., 1991). These new phases indicate that the diffusion of outward oxygen into the coatings is the dominant degradation mechanism (Ohsaki et al., 1997). Therefore, the $Cu/Ti/SiO_2/Ti/TiO_2/SiO_2$ coating was thermally stable at 300 °C in air.

4. Conclusions

High-absorption solar selective absorbing coatings including purple, blue, blue green, yellow green and orange yellow with $Cu/Ti/SiO_2/Ti/TiO_2/SiO_2$ structure were prepared by magnetron sputtering method on quartz substrates. The absorptance of all the colored solar selective absorbing coatings is higher than 0.95, the thermal emissivity is lower than 0.09 at 80 °C, and the brightness is in the range of 0.38–2.91%. The thermal stability of the $Cu/Ti/SiO_2/Ti/TiO_2/SiO_2$ multilayer coatings showed the coatings were thermally stable up to near 450 °C in vacuum and 300 °C in air for 2 h. The degradation of multilayer solar selective absorbing coatings was mainly due to diffusing the copper and subsequently oxidizing in vacuum, and the diffusing outward oxygen into the coatings in air. Furthermore, the changes of the chemical composition were confirmed by Raman spectroscopy at different temperature. Therefore, this report may provide an instruction to design and fabricate high performance colored solar selective absorbing coatings, which were applied in domestic solar water heater, space heating and energy-efficient buildings.

Table 3
Effect of 2 h annealing in air on the absorptance (α), emissivity (ε) and color change (ΔE^*_{uv}) of the blue coatings.

Annealing temperature (°C)	As-deposited		Annealed		$\Delta\alpha$	$\Delta\varepsilon$	ΔE^*_{uv}
	α	ε	α'	ε'			
300	0.964	0.079	0.963	0.088	−0.001	0.009	1.66
400	0.966	0.080	0.957	0.091	−0.009	0.011	4.18
450	0.965	0.082	0.914	0.098	−0.051	0.016	13.14
500	0.964	0.080	0.901	0.109	−0.063	0.029	32.91

Acknowledgments

This work was financially supported by the Natural Science Foundation of China (No. 11074041, 11374052), the Natural Science Foundation of Fujian Province of China (2012J01256, 2013J01174), and the Science and Technology Project from Education Department of Fujian Province of China (JB13023).

References

Anderson, T.N., Duke, M., Carson, J.K., 2010. The effect of colour on the thermal performance of building integrated solar collectors. Sol. Energy Mater Sol. Cells 94, 350–354.

Arsov, L.D., Kormann, C., Plieth, W., 1991. Electrochemical synthesis and in situ raman spectroscopy of thin films of titanium dioxide. J. Raman Spectrosc. 22, 573–575.

Biesinger, M.C., Lau, L.W.M., Gerson, A.R., Smart, R.S.C., 2010. Resolving surface chemical states in XPS analysis of first row transition metals, oxides and hydroxides. Appl. Surf. Sci. 257, 887–898.

Bostrom, T., Wackelgard, E., Westin, G., 2003. Solution-chemical derived nickel–alumina coatings for thermal solar absorbers. Sol. Energy 74, 497–503.

Boudaden, J., Oelhafen, P., Schuler, A., Roecker, C., Scartezzini, J., 2005. Multilayered Al_2O_3/SiO_2 and TiO_2/SiO_2 coatings for glazed colored solar thermal collector. Sol. Energy Mater. Sol. Cells 89, 209–218.

Chen, C.W., Chen, D.Y., Hsu, C.Y., Chang, Y.H., Hou, K.H., 2011. Spectrally selective Al/AlN/Al/AlN tandem solar absorber by inline reactive ac magnetron sputtering. Surf. Eng. 27, 616–622.

Chrzanowski, J., Irwin, J.C., 1989. Raman scattering from cupric oxide. Solid State Commun. 70, 11–14.

Kanu, S.S., Binions, R., 2009. Thin films for solar control applications. P. Roy Soc. 466, 19–44.

Kasson, J.M., Plouffe, W., 1992. An analysis of selected computer interchange color spaces. ACM T. Graphic 11, 373–405.

Lai, F., Lin, L., Gai, R., Lin, Y., Huang, Z., 2007. Determination of optical constants and thicknesses of In_2O_3 Sn films from transmittance data. Thin Solid Films 515, 7387–7392.

Li, D., Wan, D., Zhu, X., Wang, Y., Han, Z., Han, S., 2014. Broadband antireflection TiO_2–SiO_2 stack coatings with refractive-index-grade structure and their applications to Cu(In, Ga)Se_2 solar cells. Sol. Energy Mater. Sol. Cells 130, 505–512.

Lien, S., Wuu, D., Yeh, W., Liu, J., 2006. Tri-layer antireflection coatings for silicon solar cells using a sol–gel technique. Sol. Energy Mater. Sol. Cells 90, 2710–2719.

Nemanich, R., Tsai, C., Connell, G., 1980. Interference-enhanced raman scattering of very thin titanium and titanium oxide films. Phys. Rev. Lett. 44, 273–276.

Ohsaki, H., Tachibana, Y., Kadowaki, K., Hayashi, Y., Suzuki, K., 1997. Bendable and temperable solar control glass. J. Non-Cryst. Solids 218, 223–229.

Schüler, A., Roeckera, C., Boudadenb, J., Oelhafenb, P., Scartezzinia, J. L., 2005. Potential of quarterwave interference stacks for colored thermal solar collectors. Sol. Energy 79, 122–130.

Selvakumar, N., Barshilia, H.C., 2012. Review of physical vapor deposited (PVD) spectrally selective coatings for mid- and high-temperature solar thermal applications. Sol. Energy Mater. Sol. Cells 98, 1–23.

Solache-Carranco, H., Juárez-Díaz, G., Galván-Arellano, M., Martínez-Juárez, J., Romero-Paredes, G., Peña-Sierra, R., 2008. Raman scattering and photoluminescence studies on Cu_2O. Autom. Control Comp. Sci., 421–424

Tahir, D., Tougaard, S., 2012. Electronic and optical properties of Cu, CuO and Cu_2O studied by electron spectroscopy. J. Phys. – Condens. Mater. 24, 175002.

Technical Committee, ISO 10292-1994. Glass in Building-Calculation of Steady-State U Values (Thermal Transmittance) of Multiple Glazing.

Tripanagnostopoulos, Y., Souliotis, M., Nousia, T., 2000. Solar collectors with colored absorbers. Sol. Energy 68, 343–356.

Wang, R.Z., Zhai, X.Q., 2010. Development of solar thermal technologies in China. Energy 35, 4407–4416.

Wu, Y., Zheng, W., Lin, L., Qu, Y., Lai, F., 2013. Colored solar selective absorbing coatings with metal Ti and dielectric AlN multilayer structure. Sol. Energy Mater. Sol. Cells 115, 145–150.

Ye, L., Zhang, Y., Zhang, X., Hu, T., Ji, R., Ding, B., 2013. Sol–gel preparation of $SiO_2/TiO_2/SiO_2$–TiO_2 broadband antireflective coating for solar cell cover glass. Sol. Energy Mater. Sol. Cells 111, 160–164.

Zheng, M., Wu, Y., Lin, L., Zheng, W., Qu, Y., Lai, F., 2012. Design and analysis of colored solar selective absorbing films with three-layer structure. Surf. Rev. Lett. 19, 1250046.

Zheng, L., Zhou, F., Zhou, Z., Song, X., Dong, G., Wang, M., Diao, X., 2015. Angular solar absorptance and thermal stability of Mo–SiO_2 double cermet solar selective absorber coating. Sol. Energy 115, 341–346.

Zhu, D., Zhao, S., 2010. Chromaticity and optical properties of colored and black solar–thermal absorbing coatings. Sol. Energy Mater. Sol. Cells 94, 1630–1635.